Pergamon

Int. J. Solids Structures Vol. 33, No. 13, pp. 1853–1865, 1996

0020-7683/96 $15.00 + .00

0020-7683(95)00132-8

BOUNDARY ELEMENT ANALYSIS OF CRACKS

BRUCE A. AMMONS† and MADHUKAR VABLE‡
Mechanical Engineering–Engineering Mechanics, Michigan Technological University, Houghton, MI 49931, U.S.A.

(*Received* 26 *January* 1995; *in revised form* 23 *May* 1995)

Abstract—This paper presents a boundary element formulation that can be used for traction free or pressurized central, edge or branch cracks. The problems associated with the evaluation of integrals containing higher order singularities, which have forced many researchers to modify the boundary integral equations, are overcome in this paper. This permits the use of traction boundary conditions with no modification or addition to the number of unknowns. Comparison of results for conforming and non-conforming elements in modeling of cracks reveals that the oscillation in stresses near the crack tip for non-conforming elements used in the past makes the stress intensity factor dependent on the points used in its calculation. Stress intensity factors are calculated using three different methods. Numerical results for central, edge and branch cracks validate the ideas presented in this paper.

1. INTRODUCTION

The boundary element method has proven to be an effective technique for calculating stresses, displacements and stress intensity factors in crack analysis. Most of the formulations in the literature (Portela *et. al.*, 1992; Sur and Altiero, 1988; Cruse, 1988; Crouch, 1976) are for the direct version of the boundary element method. Another common feature of the published work is the use of numerical integration schemes for evaluating the integral equations. The reliance on numerical integration has forced the authors of published work to devise schemes that overcome the problems associated with the second order singularities that arise in the integral equations. Boundedness of stresses at points other than the crack tips requires that the density function and its first derivative must be continuous. This continuity requirement, particularly for the derivative of the density function, has often been ignored at the element end points and in this sense the published work shows use of only non-conforming elements in crack analysis.

In this paper a formulation based on the indirect boundary element method is presented. The crack is modeled using displacement discontinuity and the associated fundamental solution. For interior cracks the adaptation of ideas of direct BEM to indirect BEM is straight forward, but for edge cracks the interaction between the density function used for modeling the crack and the density function used for modeling the boundary causes severe numerical perturbations. The source of these numerical perturbations is explained and the problem is rectified by introducing an element that extends outside the real body. In the analysis of branch cracks the various density functions used in modeling each branch are related at the branch point. The relationship between the density functions at the branch point reported in this paper is different than that published by Liu and Altiero (1991). The higher order singularities require no separate schemes as the integration is done analytically. The analytical integration uses an iterative algorithm that is valid for any order of polynomial approximation as described in the second author's earlier works (Vable, 1985; Vable and Zhang, 1992). Conforming and non-conforming elements are used for modeling the crack. Stress intensity factors are calculated using the J-integral, least square, and crack opening displacement methods. Numerical results for straight, edge and branched cracks show good correlation with analytical results.

† National Science Foundation Graduate Research Fellow.
‡ Author for correspondence.

2. BOUNDARY INTEGRAL EQUATIONS

The integral equations are formulated using the singular solutions associated with a point force F_k and a point displacement discontinuity c_k. Let $(uF)_{ik}(P, S)$ represent the displacement u_i at the field point P due to a unit value of F_k applied at the source point S. Similarly, let $(uc)_{ik}(P, S)$ represent the displacement u_i at the field point P due to a unit value of c_k applied at the source point S.

By distributing the point force F_k on the boundary Γ_B and the displacement discontinuity c_k on the crack boundary Γ_C we obtain by superposition:

$$u_i(P) = \oint_{\Gamma_B} (uF)_{ik}(P, S)F_k(S)\,ds(S) + \int_{\Gamma_C} (uc)_{ik}(P, S)c_k(S)\,ds(S) \tag{1}$$

The boundary Γ_B represents the boundaries of the body, which can be simply or multiply connected. The crack boundary Γ_C represents the path of one or more cracks, which can be smooth, kinked, branch, or edge cracks. Similarly, the stress equation can be written as:

$$\sigma_{ij}(P) = \oint_{\Gamma_B} (\sigma F)_{ijk}(P, S)F_k(S)\,ds(S) + \int_{\Gamma_C} (\sigma c)_{ijk}(P, S)c_k(S)\,ds(S) \tag{2}$$

where $(\sigma F)_{ijk}$ and $(\sigma c)_{ijk}$ are obtained by differentiation of $(uF)_{ik}$ and $(uc)_{ik}$ with respect to the field point P.

Let the displacement and traction boundary conditions be given as:

$$u_i(P) = \bar{u}_i(P) \tag{3}$$

$$\sigma_{ij}(P)n_j(P) = \bar{t}_i(P) \tag{4}$$

where $n_j(P)$ are the direction cosines of the unit normal at point P on Γ_B or Γ_C. The unknown density functions for F_k and c_k are determined by satisfying equations (3) or (4) with P on Γ_B, and zero traction when P is on Γ_C. The influence function $(\sigma c)_{ijk}$ has a second order singularity when P is on Γ_C in equation (2). Sur and Altiero (1988) addressed the problem of the higher order singularity by transforming equation (2). The transformation may be derived by multiplying eqn (2) by n_j and integrating from infinity to some point P to obtain

$$\Pi_i(P) = \oint_{\Gamma_B} (\Pi F)_{ik}(P, S)F_k(S)\,ds(S) + \int_{\Gamma_C} (\Pi c)_{ik}(P, S)c_k(S)\,ds(S) \tag{5}$$

In writing the above equation it is assumed that the body is in equilibrium and the function Π_i is zero at infinity. The function Π_i represents the integration of traction on the arc between a point at infinity and point P. Now consider the integration of the traction along the boundary from point P_0 to P. $\Pi_i(P)$ can be written as

$$\Pi_i(P) = \Pi_i(P_0) + \int_{P_0}^{P} t_i\,ds \tag{6}$$

where $\Pi_i(P_0)$ represents the integration of traction from infinity to point P_0 and is an unknown constant that will be determined from the boundary conditions. For each continuous boundary segment on which t_i is specified, there will be a different point P_0 with a different unknown constant $\Pi_i(P_0)$.

Sur and Altiero (1988) use eqn (6) when P is on Γ_C. In this paper boundary conditions given by both equations (4) and (6) are considered. The higher order singularity poses no special difficulty due to the recursive analytical integration scheme used in this paper.

3. EDGE CRACK

The density function F_k represents the jump in traction t_k as one crosses the boundary Γ_B from the interior to the exterior of the body. Similarly, the density function c_k represents the jump in the value of displacement u_k as one crosses the crack from one side to the other. To understand the interaction of these two density functions near the edge crack, consider Fig. 1. As one moves along the crack, the density function c_k has a finite value in the interior that should go to zero in the exterior to reflect that there is no crack in the exterior. This generates large stress gradients in the exterior at the crack opening which are reflected in the exterior tractions and hence in F_k. Though it is possible to model these large gradients in F_k by making a fine mesh near the crack opening, it is a needless use of computer resources to model an artifact of the method. A simpler solution is to extend the crack into the exterior and model it with a single element. Good correlation with analytical results is obtained by extending the crack by five crack lengths into the exterior and modeling it using a single element with a linearly varying density function which equals the value and slope at the crack end as shown in Fig. 1. When extending a large crack into a hole the extension is stopped at the center of the hole, which is as far from the boundary as possible. The extension introduces no additional unknowns.

4. BRANCH CRACK

Let the density function $c_k = u_k^+ - u_k^-$ where u_k^+ and u_k^- represent the displacement on the right and left surfaces respectively as one moves along the crack in the direction of integration in eqn (1). Three crack segments forming a branch point with displacements on each side of the crack are shown in Fig. 2. Continuity of displacements at corners A, B, and C requires

$$u_k^{1+} = u_k^{2-} \qquad u_k^{2+} = u_k^{3-} \qquad u_k^{3+} = u_k^{1-} \tag{7}$$

It may be verified by substitution that the following relationship is true.

$$(u_k^{1+} - u_k^{1-}) + (u_k^{2+} - u_k^{2-}) + (u_k^{3+} - u_k^{3-}) = 0 \tag{8}$$

$$c_k^1 + c_k^2 + c_k^3 = 0 \tag{9}$$

In writing eqn (9) it was assumed that integration on each branch started at the branch point. This requirement can be dropped by defining the starting point as positive and ending point as negative. The implication of eqn (9) can be better understood by an analogy interpreting the density function as a current in an electrical circuit. The total current

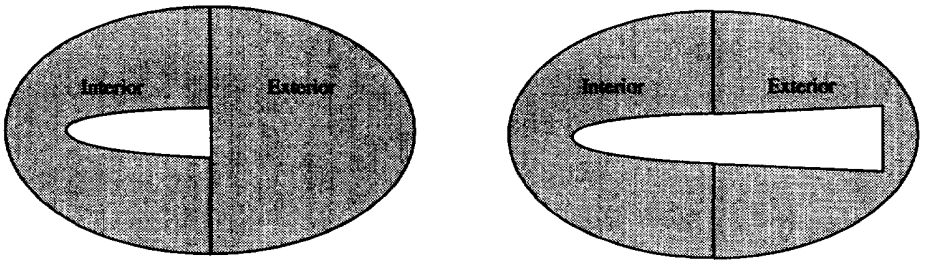

Fig. 1. Edge crack without extension and with linear extension.

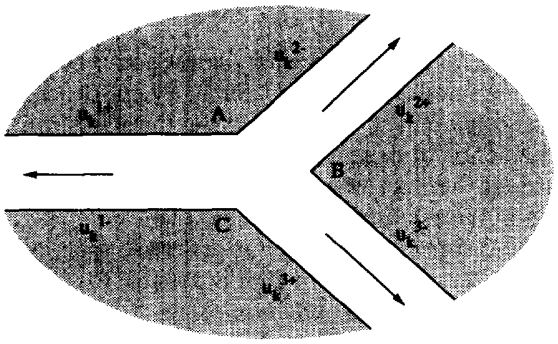

Fig. 2. Displacements at the branch point of a branch crack.

(density function) flowing into a junction (branch point) is equal to the total current flowing out.

The value of Π_i at the branch point P_J is the same irrespective of the path used to reach it. Let P_1, P_2 and P_3 be the starting points for integration for the three branches shown in Fig. 3. Equation (6) can be written for each branch as

$$\Pi_i(P_J) = \Pi_i(P_1) + \int_{P_1}^{P_J} t_i \, ds = \Pi_i(P_2) + \int_{P_2}^{P_J} t_i \, ds = \Pi_i(P_3) + \int_{P_3}^{P_J} t_i \, ds \tag{10}$$

Consider eqn (6) for point P on branch 2 starting from point P_2. The integration constant $\Pi_i(P_2)$ can be solved in terms of $\Pi_i(P_1)$ and substituted to obtain the following.

$$\Pi_i(P) = \Pi_i(P_2) + \int_{P_2}^{P} t_i \, ds = \Pi_i(P_1) + \int_{P_1}^{P} t_i \, ds \tag{11}$$

Equation (11) implies that for pressurized cracks we can use a single unknown constant but we must specify the value of integrated traction for all branches starting from the same reference point.

Liu and Altiero (1991) presented conditions on c_k and Π_i which are different from those presented in this paper. It is the author's opinion that the conditions presented by Liu and Altiero are only valid for kinked cracks that are traction free. Equations (9) and (11) are more general and valid for any number of branches with or without tractions.

5. STRUCTURE OF FUNDAMENTAL SOLUTIONS

Most fundamental solutions for isotropic bodies are a linear combination of four singular functions and a polynomial function (see Vable, 1985; Vable and Zhang, 1992) as given below.

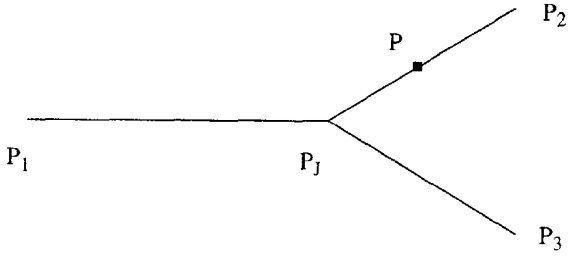

Fig. 3. Branch crack condition.

$$\text{jxy}^{i,j} = \text{Re}\left[\frac{(r_x+\bar{i}r_y)^i}{(r_x-\bar{i}r_y)^j}\right] \quad \text{kxy}^{i,j} = \text{Im}\left[\frac{(r_x+\bar{i}r_y)^i}{(r_x-\bar{i}r_y)^j}\right]$$

$$\text{lxy}^{i,j} = (r_x)^i(r_y)^j \log(r) \quad \text{txy}^{i,j} = (r_x)^i(r_y)^j \operatorname{atan}\left(\frac{r_y}{r_x}\right)$$

$$\text{pxy}^{i,j} = (r_x)^i(r_y)^j \tag{12}$$

where

$$r_x = x(P)-x(S) \quad r_y = y(P)-y(S) \quad r^2 = r_x^2+r_y^2 \quad \bar{i} = \sqrt{-1}$$

In appendix A the fundamental solutions used in this paper are given in terms of the above functions. The structure is exploited in the development of the recursive analytical integration scheme detailed briefly in this paper.

6. PROBLEM DISCRETIZATION

The integral expressions in eqns (1), (2) and (5) are reduced to algebraic expressions with the following assumptions.

1. Assume that the density functions can be represented by polynomials over M elements. The total number of unknowns generated depends upon the polynomial order and the degree of function continuity required at each end of the mth element.
2. Assume that each of the mth elements can be represented by N_m straight line segments that are tangential to the boundary. This assumption does not increase the number of unknowns but models the curvature of the boundary more accurately.

The polynomials are expanded by Taylor series about the midpoint of each segment. The assumptions reduce the problem of integration in equations (1), (2) and (5) to the evaluation of the following integral.

$$\text{Gxy}^{k,i,j} = \int_{-L/2}^{L/2} t^k \text{gxy}^{i,j}\, \text{d}t \tag{13}$$

where $\text{gxy}^{i,j}$ is one of the five functions given by equation (12) and the integration is over straight line segments. The integrals can be evaluated analytically by the recursive algorithm given in Vable (1985) for any order of polynomial (k) with any integer order of singularity ($j-i$) in the influence functions. This recursive analytical integration scheme is also used to evaluate the singularity contribution by constructing an epsilon segment with the singular point in the center. The difficulties associated with higher order singularities with numerical integration have not been encountered with the recursive analytical integration scheme described above.

An algorithm (Ammons and Vable, 1995) evaluates the coefficients of interpolation polynomials based on user specified polynomial order and continuity requirements at the end points. This algorithm provides the flexibility to choose conforming or non-conforming elements for use with any integer order of singularity in the influence functions.

7. STRESS INTENSITY FACTORS

Stress intensity factors are calculated using three different methods. (i) By the J-integral method as used by Portela *et al.* (1992) in BEM. This scheme was modified slightly to incorporate the tractions on the surface of a pressurized crack. (ii) Using the crack opening displacement method, based on the value of c_k near the crack tip, as used by Sur and Altiero (1988) in BEM. (iii) By using four terms of a series solution for stresses near the crack tip,

as used by Miskioglu *et al.* (1987) for experimental calculation of stress intensity factors, in conjunction with the least square method. A simplified representation of the series is given in Appendix B.

The J-integral method requires the evaluation of additional integral expressions for the displacement gradients. The crack opening displacement method depends on the polynomial approximation and the location of the node. The least square method overcomes the shortcomings of the above two methods, however it is more sensitive than the J-integral to the points used in the calculation. However, if the points are chosen as described in the examples, then the three methods produce comparable results.

8. RESULTS

Three numerical examples validate the ideas described in this paper. A circle with 25 points at equally spaced angular intervals in conjunction with the trapezoidal rule is used for numerical evaluation of the J-integral. The radius of the circle is chosen slightly larger than the distance where the numerical perturbations in tractions near the crack tip die out as demonstrated in example 1. In the least square method three circular arcs symmetrically placed with respect to the crack tip and subtending an angle of 240° are used for determining the stress intensity factors. Each arc has nine equally spaced points for a total of 27 sample points at which stresses are found and used for determining the 12 constants by the least square method. The stress intensity factors are compared with known analytical values.

Example 1 : *Pressurized straight crack in an infinite medium*

A crack of 2 units length has a uniform compressive pressure of 1 unit. This simulates the classic problem of a crack in an infinite medium subjected to a uniform tensile normal stress perpendicular to the crack. The problem is solved in the following three ways.

(i) c_k is approximated by piecewise continuous linear functions that are forced to zero at the crack tips. Integrated traction boundary conditions given by eqn (5) are used. A total of 52 unknowns is used for modeling the crack. This approximation is similar to that reported by Sur and Altiero (1988) for the direct method.

(ii) c_k is approximated by piecewise quadratic functions that are discontinuous at each element end and are not forced to zero at the crack tips. Traction boundary conditions given by eqn (4) are used. A total of 54 unknowns is used for modeling the crack. This approximation is similar to that used by Portela *et al.* (1992) for the direct method.

(iii) c_k is approximated by cubic hermite polynomials that ensure function and derivative continuity at each element end, and the value of c_k is forced to zero at the crack tips. Traction boundary conditions given by eqn (4) are used. A total of 52 unknowns is used for modeling the cracks. This approximation uses fully conforming elements with second order singularities.

Figure 4 shows the variation of traction starting at the crack tip and moving along the crack length. The theoretical value of traction should be -1 but due to numerical error the calculated value varies along the crack length. The linear and the quadratic approximations show large oscillations in the traction values near the crack tip which diminish away from the crack tip. The spikes in the traction values are due to violation of the continuity requirements at the element ends. With the cubic conforming elements the oscillations die out very rapidly and a value close to -1 is obtained after one twentieth of a crack length. It is possible that with other mesh discretizations the length over which these oscillations occur may change, but the basic conclusion that non-conforming elements introduce numerical perturbations near the points where continuity conditions are violated is unlikely to change.

The importance of the oscillations in traction shown in the figures is two fold : (a) The radii of the circles used for the J-integral and the least square methods should be selected such that the effect of the oscillations is minimal. Since the range of these oscillations is not known *a priori*, a rule of thumb is to use a circle that passes approximately through the

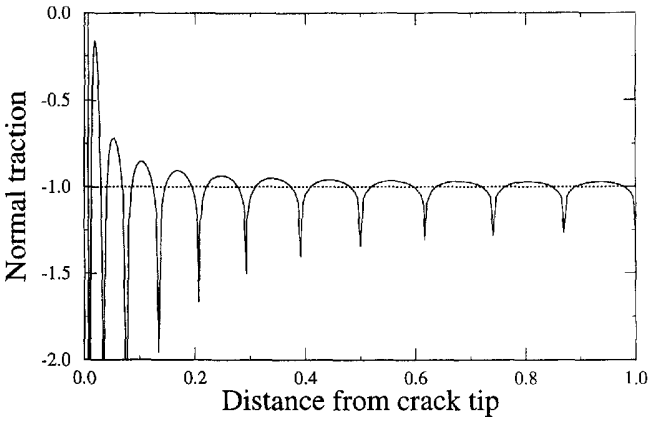

Fig. 4a. Variation of traction along surface of crack for linear elements.

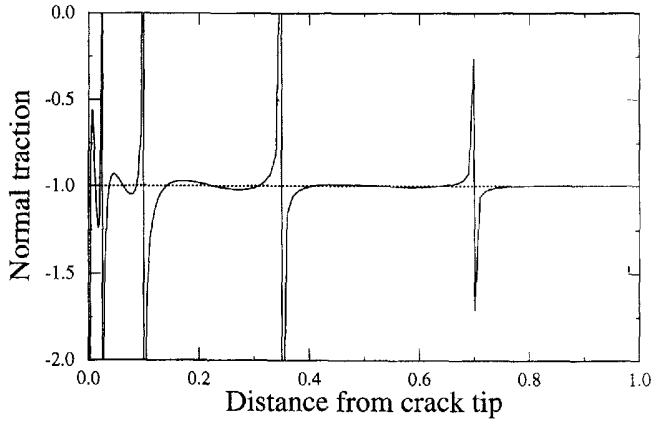

Fig. 4b. Variation of traction along surface of crack for quadratic elements.

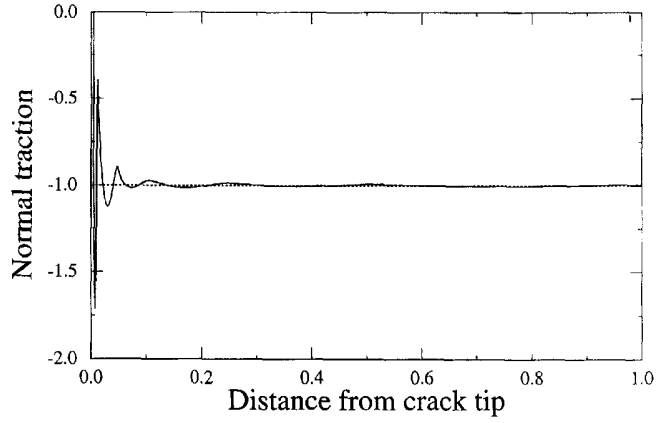

Fig. 4c. Variation of traction along surface of crack for cubic elements.

middle of the third element. The middle of the element is chosen to avoid the spikes that occur at the element ends in non-conforming elements. (b) In elastic–plastic analysis in which the stresses are found iteratively in the plastic zone at the crack tip, the use of non-conforming elements may cause severe convergence problems due to the numerical oscillations.

A circle of radius 0.15 was used to evaluate the stress intensity factor by the J-integral method. Radii of 0.12, 0.15 and 0.1875 were used in the calculation of stress intensity factors by the least square method. Table 1 shows the non-dimensionalized stress intensity factor for the three approximations. Results of all three approximations compare favorably

Table 1. Non-dimensional stress intensity factors for straight crack

Approximation	J-integral	Least squares	Unknowns	Condition number	CPU time
Linear	0.999	1.002	52	8.8	0.30 s
Quadratic	1.001	1.006	54	493.4	0.36 s
Cubic	0.999	1.001	52	613.1	0.43 s

with the theoretical value of 1.000 for the non-dimensionalized stress intensity factor. The low condition numbers shown in Table 1 are a testimony to the stability of the three approximations. The small c.p.u. times on the Sun Sparcstation IPX computer demonstrate the attractiveness of BEM for crack analysis.

Example 2: *Edge cracks*

A disc under uniform tension with an edge crack (interior problem) and a pressurized hole with an edge crack (exterior problem) are shown in Fig. 5. The dotted line represents the extension of the crack outside the body. Both problems were solved with and without the extension using 24 unknowns to model the crack and 66 to model the circular boundary. Except for the extension, the meshes were identical for all four cases studied. The objective of presenting the four cases is to demonstrate the effect of crack extension. This effect can be demonstrated adequately using the piecewise linear representation for the density functions and integrated traction boundary conditions on the crack.

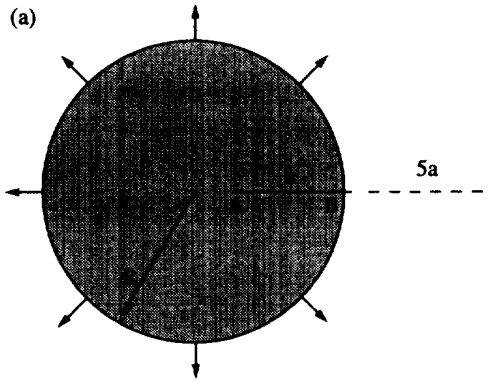

Fig. 5a. Disk with edge crack (interior problem).

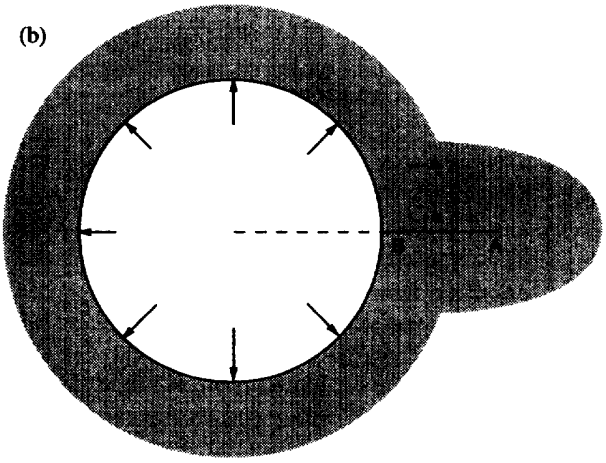

Fig. 5b. Hole with edge crack (exterior problem).

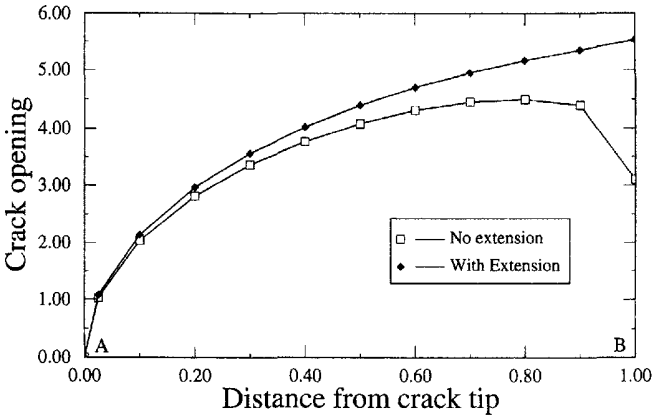

Fig. 6a. Comparison of crack opening displacements for exterior problem.

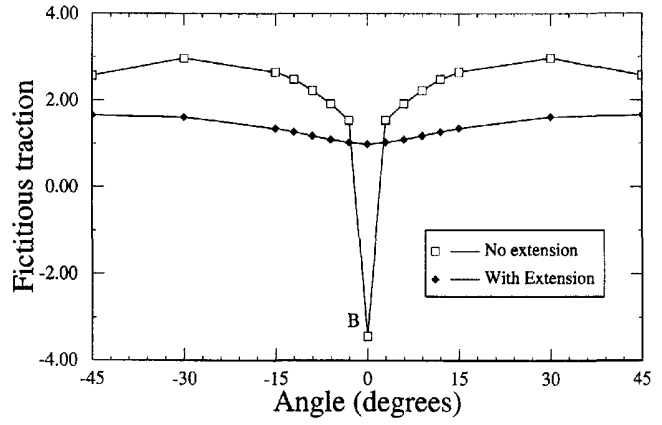

Fig. 6b. Comparison of X fictitious tractions for exterior problem.

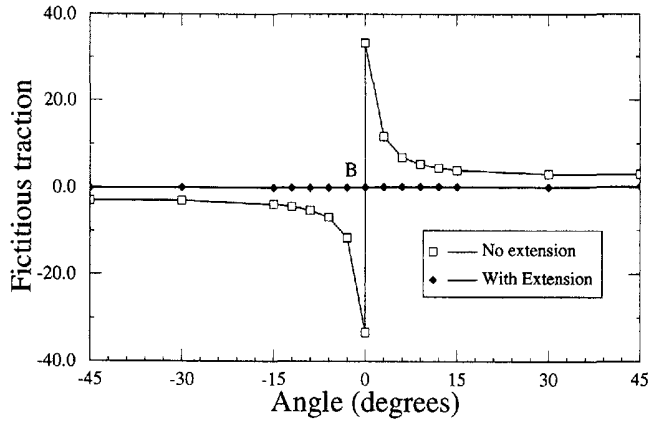

Fig. 6c. Comparison of Y fictitious tractions for exterior problem.

Figure 6a shows the crack opening displacement for the exterior problem as one moves from point A to point B. For the crack with no extension, Fig. 6a shows the trend in c_k from a finite value in the interior toward the zero value it should have in the exterior at point B. This sudden drop in c_k at point B introduces large stress gradients outside the body that are reflected as spikes in the fictitious traction density function F_k at the crack/boundary intersection shown in Fig. 6b and 6c. Figure 6a, 6b, and 6c shows that both c_k and F_k behave smoothly when the crack is extended outside the body. Similar trends were observed for the interior problem which are not presented in the paper for the sake of brevity.

Table 2. Non-dimensional stress intensity factors for hole with edge crack

a/R	Crack opening	J-integral	Least squares	Reference[a]	Condition number
1.0	1.202	1.224	1.233	1.226	1060
0.5	1.457	1.481	1.492	1.480	1846
0.1	1.935	1.971	1.984	1.988	57415

[a] Murakami (1987), 242.

Table 3. Non-dimensional stress intensity factors for disk with edge crack

a/R	Crack opening	J-integral	Least squares	Reference[a]	Condition number
1.0	3.047	3.077	3.084	3.129	646
0.5	1.722	1.749	1.758	1.739	1282
0.1	1.198	1.219	1.227	1.218	22879

[a] Tada (1973), 11.13.

The stress intensity factors for the interior and exterior problems for different ratios of crack length to the radius of the circular boundaries are presented in Table 2 and Table 3. The results are reported for solutions with crack extensions only because the results with no crack extension were found to be nonsensical. The stress intensity factors calculated from the crack opening displacement are also reported. The stress intensity factors once more show good correlation with the known analytical values. Notice the increase in matrix conditioning number as the ratio of a/R decreases. The increase in condition number is warning that very small cracks near very large boundaries may cause numerical difficulties.

Example 3: *Branch cracks*

A branch crack in an infinite plane subjected to uniform uniaxial tension σ_{yy} can be modeled as a pressurized crack with zero stresses at infinity. The geometry of the crack is shown in Fig. 7. Twenty-two elements were used on the main branch starting at A and 12 elements were used on each of the other two branches. The mesh was uniform for each branch except for the last two elements at each end of the branch. These last two elements had the length of one fourth and three fourths of the length of the uniform elements. The displacement discontinuity c_k was forced to zero at the crack tips A, B, and C. Liu and Altiero (1991) solved a similar branch crack problem, but it was enclosed in a finite rectangular body. The difference between the traction free crack of Liu and Altiero and the pressurized crack of this paper is reflected in the conditions represented by eqn (10). Stress intensity factors were calculated by the J-integral, least square, and crack opening displacement methods. Results for several b/a ratios were calculated and compared with

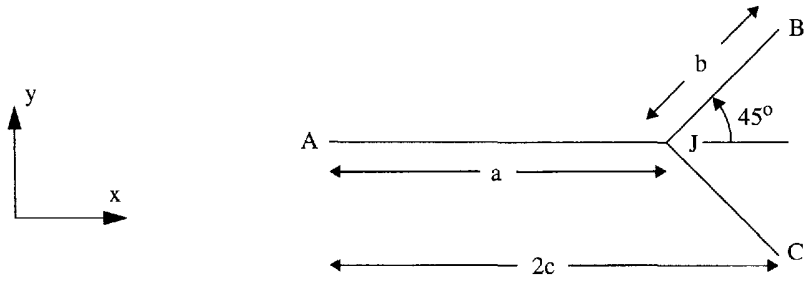

Fig. 7. Geometry of branch crack.

Table 4. Non-dimensional stress intensity factors for branch cracks

b/a		Crack opening	J-integral	Least squares	Reference[a]	Condition number
0.05	F_I^B	0.582	0.593	0.596	0.593	11.6
	F_{II}^B	0.290	0.297	0.305	0.297	
	F_I^A	0.985	1.004	1.012	1.006	
0.6	F_I^B	0.486	0.496	0.500	0.497	14.9
	F_{II}^B	0.474	0.484	0.490	0.485	
	F_I^A	1.008	1.027	1.034	1.029	

[a] Murakami (1987). 375.

analytical results reported in Murakami (1987). Results for two ratios of b/a are reported in Table 4.

Results in Table 4 show good correlation with analytical results. The condition at the junction J can be expected to affect the stresses at crack tip B for very small ratios of b/a. The good correlation of analytical and calculated results for the ratio $b/a = 0.05$ validates that the conditions at junction J given by equations (9) and (11) for pressurized cracks are correct.

The c.p.u. time on the Sun Sparcstation IPX for each ratio of b/a was 1.35 seconds. This small c.p.u. time vividly demonstrates the effectiveness of the boundary element method for branch cracks.

9. CONCLUSIONS

This paper demonstrates that the indirect boundary element method is an effective tool for the numerical analysis of deformation and stress in the vicinity of central, edge, and branch cracks that are pressurized or traction free. Results of non-conforming elements reveal that there is oscillation in stresses near the crack tip and spikes in the stresses at element ends, making the stress intensity factor very susceptible to the points used in its calculation. This oscillation problem can be alleviated by using conforming elements. The use of iterative analytical integration over each element overcomes the problems of higher order singularities reported in the past literature, permitting the use of either traction or integrated traction boundary conditions on the crack surface.

Results reported in this paper were obtained using the BEAMUP program, which is an acronym for Boundary Element Analysis from Michigan's Upper Peninsula. BEAMUP is a general purpose two-dimensional program that can solve problems in elastostatics, plate bending, or problems represented by Poisson's equation. The solution technique used by BEAMUP can be the direct or indirect BEM. The interpolation function for each element can be any order of polynomial and satisfy any order of continuity between elements. Different types of singularities with any integer order of singular behavior can be modeled by simple modification of the program. The BEAMUP program provides a common platform for comparison of different methodologies and approximations as was done in this paper.

Research is in progress to implement the ideas described in this paper for cracks at interfaces of dissimilar elastic materials.

Acknowledgement—This material is based upon work supported under a National Science Foundation Graduate Research Fellowship.

REFERENCES

Ammons, B. A. and Vable, M. (1995). Generation of interpolation functions (In preparation).

Crouch, S. L. (1976). Solution of plane elasticity problems by the displacement discontinuity method. *Int. J. Num. Methods.* **10,** 301–342.

Cruse, T. A. (1988). *Boundary Element Analysis in Computational Fracture Mechanics*. Kluwer Academic, Dordrecht.

Liu, N. and Altiero, N. J. (1991). Multiple cracks and branch cracks in finite plane bodies. *Mechanics Research Communications* **18,** 233–244.
Miskioglu, I., Mehdi-Soozani, A., Burger, C. P. and Voloshin, A. S. (1987). Stress intensity factors for near edge cracks by digital image analysis. *Engng Fracture Mech.* **27,** 329–343.
Murakami, Y. (1987). *Stress Intensity Factors Handbook*. Pergamon Press, Oxford.
Portela, A., Aliabadi, M. H. and Rooke, D. P. (1992). The dual boundary element method: Effective implementation for crack problems. *Int. J. Num. Methods* **33,** 1269–1287.
Sur, U. and Altiero, N. J. (1988). An alternative integral equation approach for curved and kinked cracks. *Int. J. Fracture* **38,** 25–41.
Tada, H. (1973). *The Stress Analysis of Cracks Handbook*. Del Research Corporation, Hellertown, Pennsylvania.
Vable, M. (1985). An algorithm based on the boundary element method for problems in engineering mechanics. *Int. J. Num. Methods* **21,** 1625–1640.
Vable, M. and Zhang, Y. (1992). A boundary element method for plate bending problems. *Int. J. Solids Structures* **29,** 345–361.

APPENDIX A. INFLUENCE FUNCTIONS

The influence functions used in this paper are described in terms of the five functions given by (12). The influence functions are for an isotropic material with plane stress, where E is Young's modulus, and v is Poisson's ratio.

Influence functions for displacements due to unit force:

$$
\begin{aligned}
(uF)_{xx} &= \frac{1+v}{8\pi E}[(1+v)\mathrm{jxy}^{1,1} - 2(3-v)\mathrm{lxy}^{0,0}] \\
(uF)_{xy} &= \frac{1+v}{8\pi E}[(1+v)\mathrm{kxy}^{1,1}] \\
(uF)_{yx} &= \frac{1+v}{8\pi E}[(1+v)\mathrm{kxy}^{1,1}] \\
(uF)_{yy} &= \frac{1+v}{8\pi E}[-(1+v)\mathrm{jxy}^{1,1} - 2(3-v)\mathrm{lxy}^{0,0}]
\end{aligned} \tag{A.1}
$$

Influence functions for stresses due to unit force:

$$
\begin{aligned}
(\sigma F)_{xxx} &= \frac{1}{8\pi}[-(1+v)\mathrm{jxy}^{1,2} - (5+v)\mathrm{jxy}^{0,1}] \\
(\sigma F)_{xxy} &= \frac{1}{8\pi}[-(1+v)\mathrm{kxy}^{1,2} + (1-3v)\mathrm{kxy}^{0,1}] \\
(\sigma F)_{yyx} &= \frac{1}{8\pi}[(1+v)\mathrm{jxy}^{1,2} + (1-3v)\mathrm{jxy}^{0,1}] \\
(\sigma F)_{yyy} &= \frac{1}{8\pi}[(1+v)\mathrm{kxy}^{1,2} - (5+v)\mathrm{kxy}^{0,1}] \\
(\sigma F)_{xyx} &= \frac{1}{8\pi}[-(1+v)\mathrm{kxy}^{1,2} - (3-v)\mathrm{kxy}^{0,1}] \\
(\sigma F)_{xyy} &= \frac{1}{8\pi}[(1+v)\mathrm{jxy}^{1,2} - (3-v)\mathrm{jxy}^{0,1}]
\end{aligned} \tag{A.2}
$$

Influence functions for displacements due to unit displacement discontinuity:

$$
\begin{aligned}
(uc)_{xx} &= -[(\sigma F)_{xxx}n_x + (\sigma F)_{xyx}n_y] \\
(uc)_{xy} &= -[(\sigma F)_{xxy}n_x + (\sigma F)_{xyy}n_y] \\
(uc)_{yx} &= -[(\sigma F)_{xyx}n_x + (\sigma F)_{yyx}n_y] \\
(uc)_{yy} &= -[(\sigma F)_{xyy}n_x + (\sigma F)_{yyy}n_y]
\end{aligned} \tag{A.3}
$$

Influence functions for stresses due to unit displacement discontinuity:

$$
(\sigma c)_{xxx} = \frac{E}{4\pi}[(-\mathrm{jxy}^{1,3} - 2\mathrm{jxy}^{0,2})n_x + (-\mathrm{kxy}^{1,3} - \mathrm{kxy}^{0,2})n_y]
$$

$$
(\sigma c)_{xxy} = \frac{E}{4\pi}[(-\mathrm{kxy}^{1,3} - \mathrm{kxy}^{0,2})n_x + (\mathrm{jxy}^{1,3})n_y]
$$

$$
(\sigma c)_{yyx} = \frac{E}{4\pi}[(\mathrm{jxy}^{1,3})n_x + (\mathrm{kxy}^{1,3} - \mathrm{kxy}^{0,2})n_y]
$$

$$(\sigma c)_{yyy} = \frac{E}{4\pi}[(\mathrm{kxy}^{1,3} - \mathrm{kxy}^{0,2})n_x + (-\mathrm{jxy}^{1,3} + 2\mathrm{jxy}^{0,2})n_y]$$

$$(\sigma c)_{xyx} = \frac{E}{4\pi}[(-\mathrm{kxy}^{1,3} - \mathrm{kxy}^{0,2})n_x + (\mathrm{jxy}^{1,3})n_y]$$

$$(\sigma c)_{xyy} = \frac{E}{4\pi}[(\mathrm{jxy}^{1,3})n_x + (\mathrm{kxy}^{1,3} - \mathrm{kxy}^{0,2})n_y] \tag{A.4}$$

Influence functions for integrated traction due to unit force:

$$(\Pi F)_{xx} = \frac{1}{8\pi}[-(1+\nu)\mathrm{kxy}^{1,1} - 4\mathrm{txy}^{0,0}]$$

$$(\Pi F)_{xy} = \frac{1}{8\pi}[(1+\nu)\mathrm{jxy}^{1,1} + 2(1-\nu)\mathrm{lxy}^{0,0}]$$

$$(\Pi F)_{yx} = \frac{1}{8\pi}[(1+\nu)\mathrm{jxy}^{1,1} - 2(1-\nu)\mathrm{lxy}^{0,0}]$$

$$(\Pi F)_{yy} = \frac{1}{8\pi}[(1+\nu)\mathrm{kxy}^{1,1} - 4\mathrm{txy}^{0,0}] \tag{A.5}$$

Influence functions for integrated traction due to unit displacement discontinuity:

$$(\Pi c)_{xx} = \frac{E}{8\pi}[(-\mathrm{kxy}^{1,2} - 3\mathrm{kxy}^{0,1})n_x + (\mathrm{jxy}^{1,2} + \mathrm{jxy}^{0,1})n_y]$$

$$(\Pi c)_{xy} = \frac{E}{8\pi}[(\mathrm{jxy}^{1,2} + \mathrm{jxy}^{0,1})n_x + (\mathrm{kxy}^{1,2} - 3\mathrm{kxy}^{0,1})n_y]$$

$$(\Pi c)_{yx} = \frac{E}{8\pi}[(\mathrm{jxy}^{1,2} + \mathrm{jxy}^{0,1})n_x + (\mathrm{kxy}^{1,2} - 3\mathrm{kxy}^{0,1})n_y]$$

$$(\Pi c)_{yy} = \frac{E}{8\pi}[(\mathrm{kxy}^{1,2} - 3\mathrm{kxy}^{0,1})n_x + (-\mathrm{jxy}^{1,2} + 3\mathrm{jxy}^{0,1})n_y] \tag{A.6}$$

APPENDIX B. SERIES SOLUTION FOR STRESSES NEAR CRACK TIP

The stresses in the vicinity of the crack tip are written as a series using polar coordinates with the origin at the tip of the crack.

$$\begin{aligned}\sigma_{11} = &\sum_{n=0}^{N} A_n r^{\lambda}[\cos\lambda\theta - \lambda\sin\theta\sin(\lambda-1)\theta] \\ &+ \sum_{n=0}^{N} B_n r^{\lambda}[2\sin\lambda\theta + \lambda\sin\theta\cos(\lambda-1)\theta] \\ &+ \sum_{n=0}^{N} C_n r^{n}[2\cos n\theta - n\sin\theta\sin(n-1)\theta]\end{aligned} \tag{B.1}$$

$$\begin{aligned}\sigma_{22} = &\sum_{n=0}^{N} A_n r^{\lambda}[\cos\lambda\theta + \lambda\sin\theta\sin(\lambda-1)\theta] \\ &+ \sum_{n=0}^{N} B_n r^{\lambda}[-\lambda\sin\theta\cos(\lambda-1)\theta] \\ &+ \sum_{n=0}^{N} C_n r^{n}[n\sin\theta\sin(n-1)\theta]\end{aligned} \tag{B.2}$$

$$\begin{aligned}\sigma_{12} = &\sum_{n=0}^{N} A_n r^{\lambda}[-\lambda\sin\theta\cos(\lambda-1)\theta] \\ &+ \sum_{n=0}^{N} B_n r^{\lambda}[\cos\lambda\theta - \lambda\sin\theta\sin(\lambda-1)\theta] \\ &+ \sum_{n=0}^{N} C_n r^{n}[-\sin n\theta - n\sin\theta\cos(n-1)\theta]\end{aligned} \tag{B.3}$$

where

$$\lambda = n - \tfrac{1}{2} \qquad A_0 = \frac{K_{\mathrm{I}}}{\sqrt{2\pi}} \qquad B_0 = \frac{K_{\mathrm{II}}}{\sqrt{2\pi}} \tag{B.4}$$